Journal of Environmental Sciences Studies

Journal home page: www.jess.ir

Equilibrium and Kinetic Study of Adsorption of Mo (VI) and Pd (II) from Aqueous Solutions by Functionalized Multi-Walled Carbon Nanotubes

Mohammad Reza Almasian[2], Hossein Sid Kalal[1]*, Mohmmad Tagiof [3]

Nuclear Fuel Research School, Nuclear Science and Technology Research Institute, AEOI, P.O. Box 11365-3486, Tehran, Iran.

*Email Address: hsidkalal@aeoi.org.ir

Received: (May-14-2021)
Accepted: (June -28-2021)

Abstract

In this work, a new type of solid adsorbent was prepared by functionalization of carbon nanotubes and the structure and morphologies of the amine-functionalized Multi-walled carbon nanotubes were characterized by Fourier transform infrared spectroscopy (FTIR), thermogravimetric analysis (TGA) and scanning electron microscope (SEM). Its adsorption behavior towards Pd(II) and Mo(VI) ions was investigated. For this purpose, a solid phase extraction process using the prepared adsorbent was carried out in the pH range of 1 to 9. The effect of various parameters such as initial concentration, time and interfering ions on the adsorption amount was investigated, and the optimal conditions for the maximum extraction of the two ions were obtained. The adsorption of these ions by the synthesized MWNTs in real samples was examined and good results were achieved. The negative value of the change in standard Gibbs free energy ($\Delta G°<0$) for Mo(VI) sorption by the adsorbent specify a spontaneous and realizable sorption process. The changes in free energy (ΔG °), enthalpy (ΔH °) and entropy (ΔS °) for Pd(II) ions associated with Mo(VI) ions are reversed. finally, The compatibility of the experimental data with the adsorption isotherms of Langmuir, Freundlich and Redlich-Peterson were investigated for the adsorption of Mo(VI) and Pd (II) the modified carbon nanotubes.

Keywords

Adsorption; amine-functionalized MWNT; Kinetic Study.

Introduction

Given the importance of Pd(II) and Mo(VI) ions in nuclear waste, research is valuable and important to suggest new methods for extracting and separating these ions.Palladium is a rare silver and white metal from the platinum group. Palladium (Pd) is chemically similar to platinum, is extracted from copper and nickel ores and is used to manufacture industrial catalysts and jewelry. This metal, with its low density, has the lowest melting point among the metals of the platinum group and combines strongly with sulfuric and nitric acids and slowly dissolves in hydrochloric acid. Pd does not combine with oxygen at normal temperatures. It is found along with platinum, copper, and mercury minerals. Natural palladium isotopes consist of six isotopes. The most stable radioactive isotopes of the metal is Pd-107, with a half-life of 6.5 million years. The Pd-103 has a half-life of 17 days and the Pd-100 has a half-life of 3.63 days. Another 18 radioactive isotopes are classified according to their atomic weight. With the exception of Pd-101 with a half-life of 8.47 hours, Pd-109 with a half-life of 13.7 hours, and Pd-112 with a half-life of 21 hours, the other unstable isotopes of this metal have a half-life of less than half an hour [**1-6].**The abundance of molybdenum in the earth's crust is 0.007%. Molybdenum (Mo) is a white or off-white metal and its mineral is molybdenite (MoS_2), which is an essential element for plant nutrition.Molybdenum is insoluble in hydrochloric acid, sodium hydroxide, ammonia and sulfuric acid and reacts with hot or concentrated sulfuric acid or nitric acid and boiling hydrochloric acid. Studies of the environmental hazards of molybdenum have shown that it is generally one of the most dangerous substances that can cause acute poisoning when consumed. Molybdenum can cause severe gastrointestinal irritation with diarrhea, coma, and death from heart failure. When it is absorbed into the skin, it is very harmful and irritating to the skin. It also affects the nervous system, lungs, and respiratory tract, and can cause skin allergies and severe damage to the skin, eyes, and airways. Molybdenum is used in the aerospace, automotive and electronics industries. Beans need molybdenum to remove bacterial nitrogen. Approximately 25 to 75% of the molybdenum in food is absorbed by the gastrointestinal tract and quickly excreted in the urine. Animal data show that the metabolism of molybdenum

compounds is closely related to the metabolism of copper and sulfur compounds [7-11].In recent years, various methods have been proposed to eliminate metal ions, such as chemical precipitation, reverse osmosis, electrolytic recycling, ion exchange or adsorption by various adsorbents. The adsorption process is widely used because of its simplicity and cost-effectiveness. Various sorbents such as seaweed, crab skin, dry activated sludge and activated carbon made from almond kernels have been used to remove metal ions from water. The effect of particle size of the adsorbent was discussed and a direct relationship between particle size and adsorption rate was obtained and researchers became aware of the ability of nanoparticles as adsorbents for the pollutant materials. For this purpose, many studies on the application of carbon nanotubes to remove metal ions have been carried out over the past ten years [12-20].

2. Materials and Methods

2.1. **Chemicals and materials**

All materials used in this project such as $Na_2MoO_4.2H_2O$, $PdCl_2$, $CdSO_4$, BaCl2, $NiCl_2$, CaH_2 ,$FeSO_4.14H_2O$, HCl ,NH4NO3, Ethylenediamine with a purity of 99% and thionyl chloride with a purity of 99% are provided by one of the companies Merck, Fluca or Sigma Aldrich. Purified multi-walled carbon nanotubes (MWNTs): Carbon content: >97%; CNT content: >95%; Outer Diameter:<8nm Inner Diameter：2-5nm; Length：10-30um; is purchased from Chengdu Organic Chemicals Co.Ltd.,Chinese Academy of Sciences.

2.2. **Synthesis of amine-functionalized** MWNTs

In order to prepare the MWNT-COOH, raw MWNTs (0.54 g) were added to a mixture of sulfuric acid and nitric acid in a volumetric ratio of 3:1 and stirred in an ultrasonic bath (40 kHz) for about 30 minutes while it was refluxed. Then the solution was washed with distilled water until the pH of the filtrate reached approximately seven. The obtained material was dried under vacuum at 60 ° C for 12 hours to give COOH-functionalized MWNT. Then 0.5 g of MWNT-COOH in 30 ml of thionyl chloride was exposed and stirred at 65 ° C for 24 hours and then filtered, washed with anhydrous tetrahydrofuran and dried under vacuum at 25 ° C for 24 hours. The yield of MWNT-COCl was obtained. Then 0.48 g of acyl chloride-functionalized MWNT in 20.0 ml of $C_2H_8N_2$ were exposed to an ultrasonic bath (40 kHz) at 60 ° C for 5 hours and the solution was then stirred at 60 ° C for a further 24 hours. The yield obtained was collected by vacuum filtration followed by washing with anhydrous methanol. After repeated washing and filtering, the resulting crop was dried in a vacuum for 24 hours to give amine-functionalized MWNT (Figure 1).

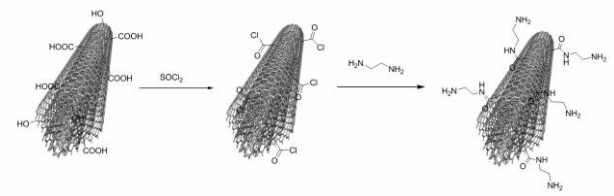

Figure 1. The schematic synthesis of the amine functionalized MWNTs.

2.2. Adsorbent Characterization

2.2.1. FTIR analysis

The use of infrared spectrum is one of the most common methods for investigating the functionalization of carbon nanotubes. In this study, the infrared spectrum of pristine nanotubes and functionalized nanotubes has been obtained by an FTIR device model Vector22 made in Bruker Company of Germany. The sampling method was potassium bromide tablets.

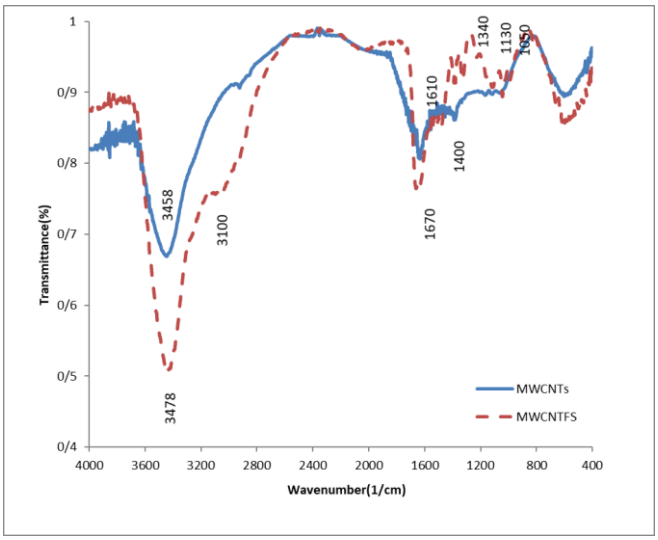

Figure 2. FTIR spectrum of MWCNTs and MWCNTFs.

Figure. 2 shows the pronounced peak developments and the peak in the range of 1670 cm^{-1} belongs to carbonyl group. The peak in 1051 cm^{-1} can be related to C-O, whose presence indicates the formation of the carboxyl functional group.From the comparison of the two spectra, the creation of new functional groups that have formed some new absorption peaks in the spectrum is clear. In the spectrum of the adsorbent, around a wavelength of 3100 cm^{-1}, a small wide peak is observed, which can be related to the tensile adsorption of the N – H bond. An absorption peak of about 3478 cm^{-1} is also observed in functionalized nanotubes, which can be due to the integration of the absorption band of the O-H group and the tensile adsorption of NH2. The peak of 1660 cm^{-1} in the primary nanotube can be related to the C = C bond in its structure, which after being actuated by a relatively wide peak in the range of 1670 cm^{-1} of the carbonyl amide group is covered.

2.2.2. Thermal Gravimetric Test (TGA).

The TGA thermograms of the primary nanotube are shown in Figure 3A and the thermograms of the functionalized nanotubes are shown in Figure 3B. These thermograms were performed under the inert gas of argon from ambient temperature to 800 °C at a rate of 10 °C per minute. As can be seen in these figures, the functionalized nanotube has lost weight in three stages before the temperature of 500 degrees, but in the initial nanotube, the main weight loss occurs at about 550 °C and with a steep slope. This observation is consistent with the presence of significant functional groups on the surface of the synthesized nanotubes.

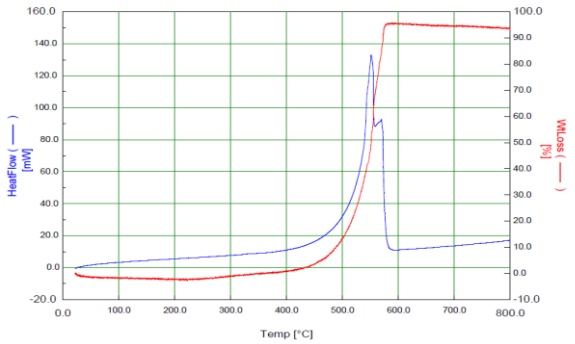

(A)

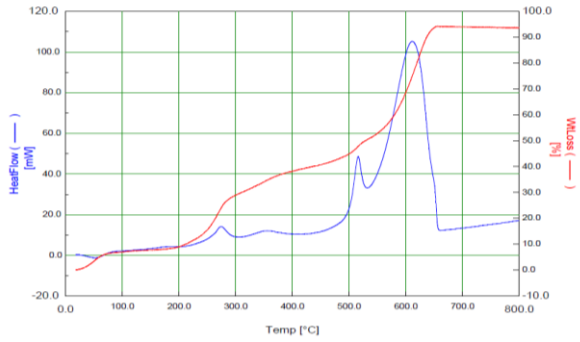

(B)

Figure 3. Thermal Gravimetric Test (TGA) of MWCNTs (A) and MWCNTFs (B).

2.2.3. Scanning electron microscopy (SEM) examinations

The SEM image of the primary nanotube is shown in Figure 4A and the SEM images of the functionalized nanotubes are shown in Figures 4B and C. As can be seen from these photos, it can be said that the functional groups have almost uniformly covered the surface of the nanotubes.

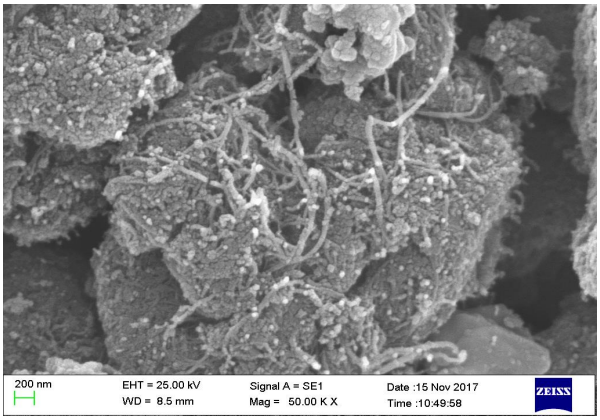

(A)

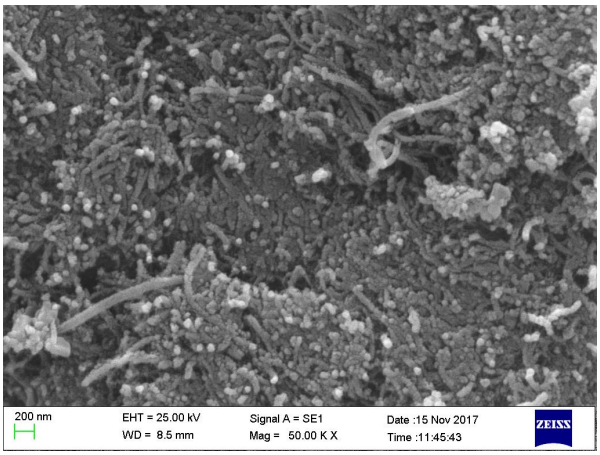

(B)

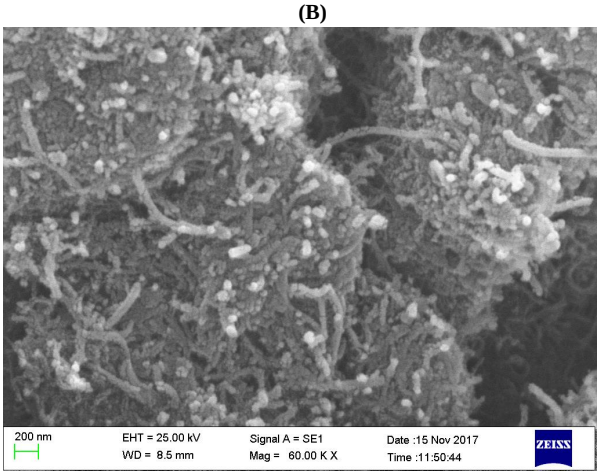

(C)

Figure 4. SEM images of MWCNTs (A) and MWCNTFs (B and C).

3. RESULTS

3.1. Effect of pH

The initial pH of the solution may be considered as one of the most important parameters in the adsorption of metal ions. The pH estimates the net charge on the sorbent which invariably determines whether the ions can bind . To determine optimum pH for maximum adsorption of molybdenum ions, seven 25 mL polyethylene tubes containing 0.01g adsorbent and 2mg/ L concentration of molybdenum solution were prepared. The acid or base was used to adjust the pH from 1 to 9. After that, all the samples were placed in an ultrasonic instrument for 30 seconds as long as they became in similar phase, and then they were placed in a thermostatic shaker bath for 3.5 hr. After filtering the adsorbent, the concentration of residual Mo(VI) ions solutions was measured by the ICP instrument. All the above stages were repeated for Pd(II) ions solutions. In this case, the pH values were from 3 to 9. As indicated in Figure 5, the best pH values for Mo(VI) and Pd(II) were 3 with adsorption of 74 % and 6 with adsorption of 84.32 %, respectively. The adsorption percentage of Mo(VI) and Pd(II) increases gradually from initial pH, reaches to a maximum value and thereafter decreases.

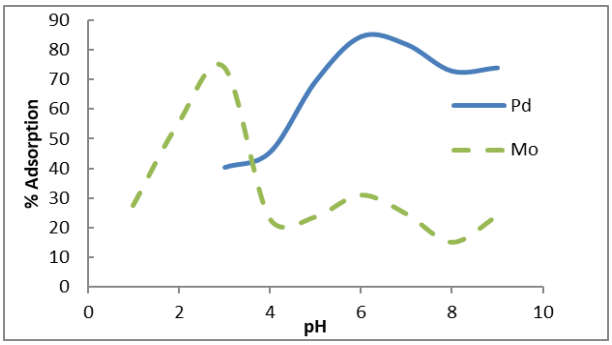

Figure 5. The effect of pH on the percentage of amounts adsorption of Mo(VI) and Pd(II).

3.2. Effect of initial metals ions concentration

Six different concentrations in the range of 0.5 to 3 mg/ L at intervals 0.5 mg/ L in 25 mL Mo(VI) ions solutions with 0.01g adsorbent were used at the best pH value. They were placed in a thermostatic shaker bath for 3.5 hr. After filtering the adsorbent, the concentration of residual Mo(VI) and Pd(II) ions in the solutions was measured by the ICP instrument. As shown in Figure 6, the best initial ion concentration values for Mo(VI) and Pd(II) are 1 mg/ L with adsorption of 72.8 % and 2 mg/ L with adsorption of 85 %, respectively.

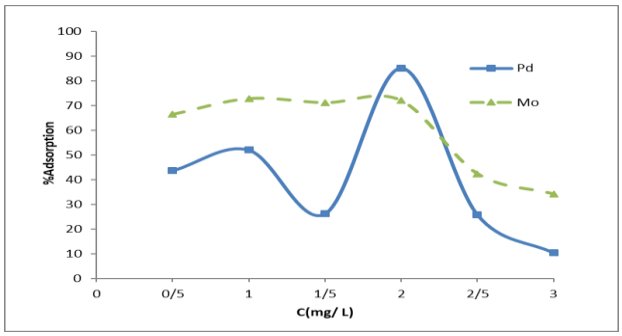

Figure 6. The effect of various initial concentrations on adsorption

3.3. Effect of the adsorption time.

The adsorption experiment was performed at different times (5, 10, 15, 30, 45, 60, 75, 90, and 120 min). 0.01 g adsorbent was added to 25 mL solution containing 1 mg/L of Mo(VI) (and 2 mg/L for Pd(II)) at the best pH value. After filtering the adsorbent, the concentration of the ions was determined by the ICP-AES . The adsorption is as an exponential function of contact time. The adsorption percentage will be increased with increasing time, as shown in Figure 7.

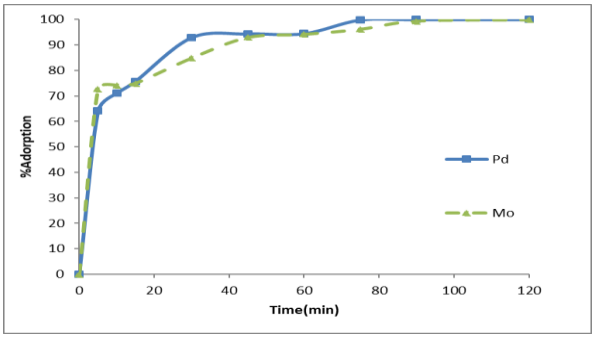

Figure 7. The effect of contact time on the adsorption

3.4. Effect of temperature

The adsorption capacity was investigated at various temperatures (20, 30, and 40 °C) and initial concentrations of 0.5, 1, 2, 4, 6, 8, 10 mg/ L at the best pH values, as shown in Table 1 and Figure 8.In all experiments, volume of solution and amount of adsorbent were 25 mL and 0.01 g, respectively. After that, all the samples were placed in an ultrasonic instrument for 30 seconds, and then they were placed in a thermostatic shaker bath for 3.5 hr at the various temperatures. After filtering the adsorbent, the concentration of residual ions solutions was measured by the ICP instrument.

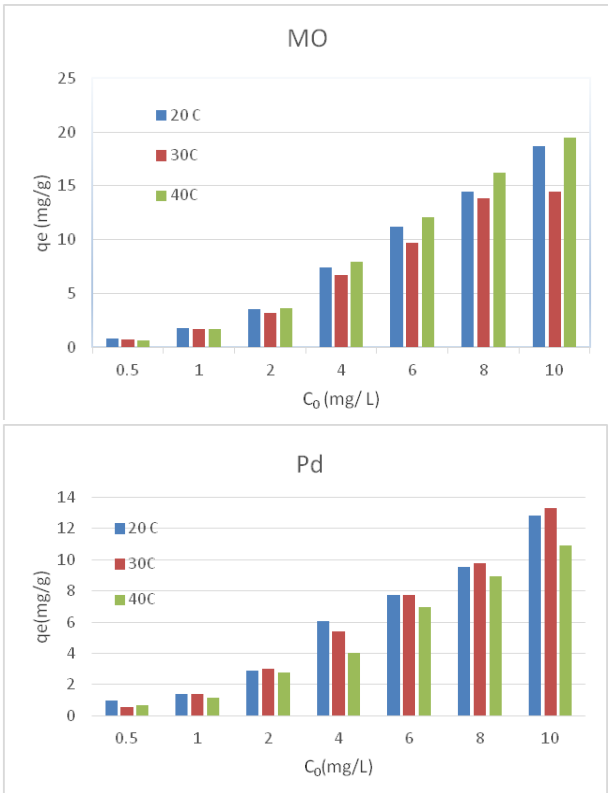

Figure 8. the effect of time and initial concentration of Mo(VI) and Pd(II) ions on the adsorption capacity.

Table 1. Equilibrium results with Mo(VI) and Pd(II) ions with initial concentrations from 0.5 to 10 mg/L and Temperatures of 293, 303 and 313 k.

Temperatures									
Mo(VI) and Pd (II) ions	**T=293k**			**T=303k**			**T=313k**		
C_0(mg/ L)	Ce	Kd	q	Ce	Kd	q	Ce	Kd	q
	mg/L	(L/g)	mg/g	mg/L	(L/g)	mg/g	mg/L	(L/g)	mg/g
0.5	0.18	0.711111	0.81	0.22	0.509091	0.71	0.24	0.433333	0.66
	0.1	1.6	0.99	0.27	0.340741	0.58	0.23	0.469565	0.68
1	0.29	0.97931	1.77	0.31	0.890322	1.73	0.33	0.812121	1.68
	0.45	0.488889	1.37	0.44	0.509091	1.41	0.53	0.354717	1.17
2	0.56	1.028572	3.60	0.73	0.69589	3.18	0.55	1.054546	3.62
	0.85	0.541176	2.87	0.8	0.6	3.01	0.89	0.498876	2.78
4	1.04	1.138462	7.40	1.30	0.830769	6.75	0.82	1.55122	7.95
	1.57	0.619108	6.09	1.85	0.464865	5.39	2.4	0.266667	4.01
6	1.53	1.168628	11.18	2.13	0.72676	9.69	1.18	1.633898	12.06
	2.91	0.424742	7.72	2.91	0.424742	7.73	3.21	0.347664	6.98
8	2.21	1.047964	14.48	2.48	0.890322	13.81	1.51	1.719205	16.22
	4.18	0.36555	9.55	4.08	0.384314	9.8	4.42	0.323982	8.95
10	2.54	1.174803	18.65	4.20	0.552381	14.50	2.21	1.409955	19.48
	4.88	0.419672	12.81	4.67	0.456531	13.33	5.63	0.31048	10.93

- **1st row refers to Mo and 2nd row refers to P**

3.5. Desorption studies

Desorption of the adsorbed ions was evaluated by 10 ml of 1 M HNO_3, HCl, NH_4NO_3 and HNO_3 + HCl solutions. Among the various reagents used, 1 M-HCl and 1 M-HNO_3 + HCl were the most effective reagents for Mo (VI) and Pd (II) ions desorption,respectively. As indicated in Table 2, the best extraction percentages were 93% (HCL) and 88% (HNO_3 + HCl), indicating good adsorbent regeneration properties and reversibility of the adsorption process.

Table 2. The extraction percentages by using various Desorption solutions

Desorption agent	**After washing with 10 ml desorption solution**		**Percentage extraction (%)**	
Concentration 1 M	**Mo(VI) Concentration (mg/ L)**	**Pd(II) Concentration (mg/ L)**	**Mo(VI)**	**Pd(II)**
HNO_3	0.84	1.42	42.00	71.00
HCl	1.86	1.35	93.00	67.50
NH_4NO_3	1.20	1.10	60.00	55.00
HNO_3 + HCl	0.73	1.76	36.50	88.00

3.6. Effect of contact time on adsorption-desorption

Desorption process was carried out after filtering of the adsorbent and recovering of the adsorbed ions by the solvent. The volume of the solution and the amount of adsorbent were 25 mL and 0.01 g, respectively. The concentration of ions was 2 mg/L at the optimum pH. To complete the adsorption process, all the samples were placed in a thermostatic shaker bath at the speed of 180 RPM for various times of 5, 15, 30, 45, 60, 75, and 120 min. After filtering the adsorbent, the concentration of residual ions solutions was measured by the ICP instrument, as shown in Figure 9.

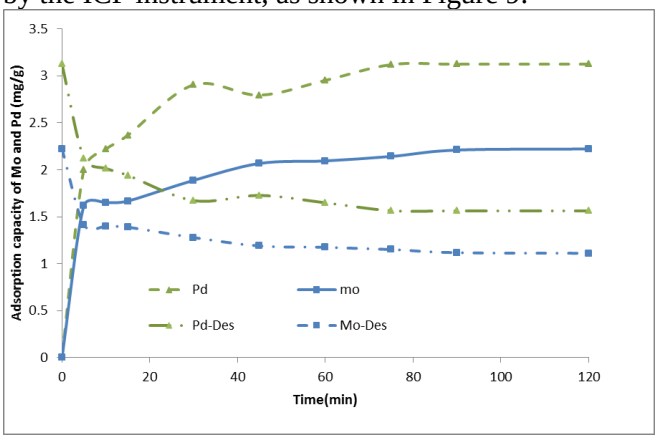

Figure 9. Mo(VI) and Pd(II) adsorption and desorption as a function of time at optimum conditions

3.7. Adsorption isotherms

Three different adsorption isotherm models with two parameters (Langmuir and Freundlich) and three parameters (Redlich-Peterson) were used to explain the equilibrium data. These models are commonly used to pre-examine the adsorption isotherm. The Langmuir model is often used for monolayer sorption, which occurs on a homogeneous surface with identical sorption sites. The equation form can be expressed by the following equation.

$$q_e = \frac{q_m K_a C_e}{1 + K_a C_e} \qquad (1)$$

Where K_a and q_m are the Langmuir constant and the maximum amount of adsorption capacity (mg/g), respectively. The q_m and C_e are equilibrium concentrations in solid and liquid phases, respectively. where C_e is the equilibrium concentration of ions remaining in the solution (mg/L), q_e is the amount of metal ions adsorbed per weight unit of the solid after equilibrium (mg/g) and q_{max} is the maximum adsorption capacity of the adsorbent (mg/g). Langmuir isotherm model is shown in Figure 10 and the value of the obtained parameters is shown in Table 3.

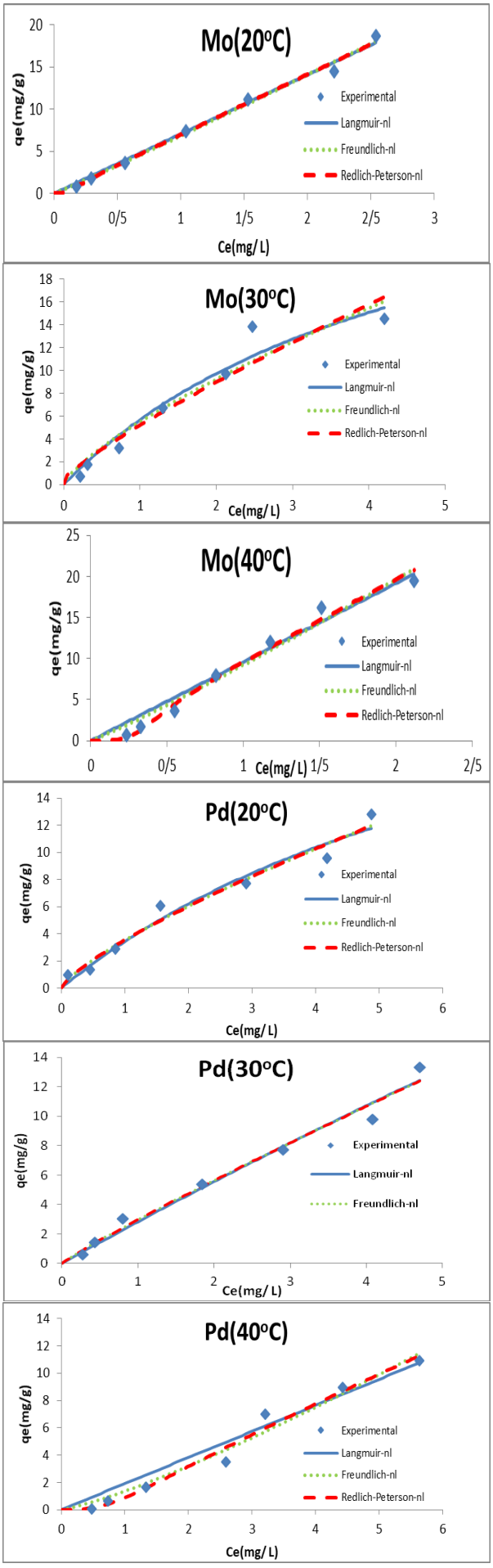

Figure 10. Best nonlinear isotherms for the adsorption of Pd(II) and Mo(VI) ions at different temperatures

Table 3. Langmuir-nl, Freundlich-nl and Redlich-pet. Isotherm constants for the adsorption of Mo(VI) and Pd(II) ions onto MWNT-NH_2

Isotherm model	T(K)	Parameters					
Langmuir-nl		q_m	k		R^2	RMSE	$(100\times\chi)^2$
	293	4.77×10^{6}	1.47×10^{-6}		0.9915	0.5775	4.1995
		31.4761	0.1227		0.9652	0.7639	9.4990
	303	33.51	0.2046		0.9492	1.1761	17.9728
		149.3368	0.0193		0.9789	0.6424	6.8832
	323	7.98×10^{5}	1.20×10^{-5}		0.9638	1.4195	10.7055
		2.6345×10^{6}	7.2530×10^{-7}		0.9538	0.6071	7.8919
Freundlich-nl		K	n		R^2	RMSE	$(100\times\chi)^2$
	293	6.8295	0.9597		0.9922	0.5547	4.0573
		3.5419	1.3028		0.9688	0.7228	7.9813
	303	5.5004	1.3402		0.9261	1.4190	26.7115
		2.9783	1.0855		0.9804	0.6210	6.7452
	323	9.2351	0.9215		0.9673	1.4306	13.1156
		1.3556	0.8096		0.9710	0.8581	6.7602
Redlich-pet.		K1	K2	g	R^2	RMSE	$(100\times\chi)^2$
	293	3.0396×10^{4}	2.1951×10^{-4}	-2.0021	0.9928	0.5604	4.0979
		6.7396×10^{-4}	7.0827×10^{-11}	0.2328	0.9688	0.7228	7.9813
	303	9.7813×10^{6}	6.7652×10^{-7}	0.2530	0.9164	1.0955	32.5617
		1.3520×10^{10}	4.5396×10^{9}	0.0788	0.9804	0.6449	6.7452
	323	9.8405	0.0280	-3.5106	0.9839	0.6203	8.89340
		2.0689	1.3720	-2.1501	0.9789	0.6554	4.9431

- 1st No. refers to Mo and 2nd No. refers to Pd

The Freundlich isotherm is a curve that corresponds to the concentration of a solute on the surface of an adsorbent to the concentration of the solute in the liquid phase. This model can be applied to multi-layer adsorption with uneven distribution of the heat and affinities of adsorption over the heterogeneous surface. It is stated as follows:

$$q_e = K_F C_e^{1/n} \qquad (2)$$

K_F and n refer to the Freundlich constants, and q_e and C_e are equilibrium concentrations in solid and liquid phases, respectively.The Redlich–Peterson isotherm is a hybrid of the Langmuir and Freundlich isotherms (Redlich and Peterson 1959). The numerator is from the Langmuir isotherm and has the benefit of approaching the Henry region at infinite dilution. The denominator has the hybrid Langmuir–Freundlich form as follows,Where q_e is equilibrium capacity, C_e is equilibrium concentration and A and B are equilibrium constants. Isotherm curves were estimated using different models (Table 3). Figure 10 suggests The Langmuir, Freundlich and Redlich Peterson isotherms at various temperatures. In order to verify the model for the adsorption system, the data must be analyzed using error analysis. Various error functions were applied in this study, namely the RMSE equation (Root-Mean-Square Error) (4) and the chi-square equation (5). A chi-square ($\chi 2$) is a test that measures how a model compares to actual observed data [21-23].

$$q_e = \frac{AC_e}{1+BC_e^g} \qquad (3)$$

$$RMSE = \sqrt{\frac{\sum_{i=1}^{n}(x_{obs,i}-x_{model,i})^2}{n}} \qquad (4)$$

$$\chi^2 = \frac{\sum_{i=1}^{n}(x_{obs,i}-x_{model,i})^2}{x_{model,i}} \qquad (5)$$

3. 8. Thermodynamic properties.

The adsorption of Mo(VI) and Pd (II) on MWNT-NH2 at different temperatures showed (Figure 8) an increase in the amount of adsorption with an increase in

temperature. The change in standard Gibbs free energy (ΔG°) is the basic criterion of spontaneity. Reactions occur spontaneously at a given temperature when ΔG° is a negative quantity. The change in free energy (ΔG °), enthalpy (ΔH °) and entropy (ΔS °) associated with the adsorption process was calculated using the following equations:

$$\Delta G^{\circ} = -RT \ln K_d \quad (6)$$

$$\ln K_d = -\frac{\Delta H^{\circ}}{RT} + \frac{\Delta S^{\circ}}{R} \quad (7)$$

$$\Delta G^{\circ} = \Delta H^{\circ} - T\Delta S^{\circ} \quad (8)$$

Where R (8.314 J/ mol· K) is the ideal gas constant; T (K) is the temperature of the solution; K_d is the linear sorption distribution coefficient. The diagrams of $\ln K_d$ versus 1/T for the adsorption of Mo(VI) and Pd(II) ions. This diagram provides the numerical values of ΔH ° and ΔS ° from the slope and the intercept. The variation in ΔG ° was also calculated based on ΔH ° and ΔS ° (see Equations 6 to 8). The value of the obtained parameters is shown in Table 4. ΔH ° and ΔS ° were 8.25 kJ /mol and 34.76 J/ mol.K for Mo(VI), respectively. The positive values of ΔH^{o} suggest the endothermic nature of the adsorption of the Mo(VI) ions on MWNT-NH2. The positive ΔS° shows the increasing randomness at the interface between solid and solution during the adsorption process. The positive ΔS° also reflects the affinity of the adsorbent for Mo(VI). The negative ΔG ° for Mo(VI) sorption by MWNT-NH2 specify a spontaneous and realizable sorption process and suggest that the modification process was effective. The changes in free energy (ΔG °), enthalpy (ΔH °) and entropy (ΔS °) with Pd (II) ions associated with Mo (VI) ions are reversed.

Table 4. Thermodynamic results of Mo(VI) and Pd(II) ions adsorption by MWNT-NH2 in temperatures of 293, 303 and 313 K.

	dG(kJ/mol)			dH (kJ/mol)	dS (kJ/mol. K)
	T=293 k	T=303 k	T=313k		
Mo	-1.94	-2.29	-2.63	8.25	34.76
Pd	-0.30	-0.08	0.46	-11.4	-37.72

3.9. Effect of interfering ions

The effect of other ions (5 mg/L) such as Ca^{+2}, Ni^{+2}, Fe^{+3}, Co^{+2}, Ba^{+2}, Cd^{+2},and Pt^{+4} on the uptake of Mo(VI) and Pd(II) (concentration 5 mg/L) was investigated.The extraction percentage (E ٪) can be calculated by the following equations, where Q is the adsorbent capacity (mg/g), the C_o and C_e stand for the initial and equilibrium concentrations (mg/L), and the W, V, and E % are the mass of adsorbent (0.01 g), the volume of solution (0.025 L), and the extraction percentage, respectively. The interfering ions have a negligible effect on the uptake, as listed in Table 5.

Table 5. Effect of interfering ions on sorption Pd(II) and Mo(VI)

Interfering Ion	A		%E		%L		D	
	Pd(II)	Mo(VI)	Pd(II)	Mo(VI)	Pd(II)	Mo(VI)	Pd(II)	Mo(VI)
-	4.09	4.71	81.88	94.26	0.00	0.00	2.05	--
Ni^{+2}	2.76	4.16	55.26	83.20	32.51	11.73	1.38	2.36
Ca^{+2}	2.90	3.97	57.96	79.48	29.21	15.68	1.45	2.08
Fe^{+3}	1.79	3.93	35.75	78.58	56.35	16.63	0.89	1.99
Ba^{+2}	1.59	4.17	31.84	83.46	61.11	11.46	0.80	1.96
Cd^{+2}	2.95	3.95	58.9	78.90	28.04	16.30	1.47	2.09
Co^{+2}	1.32	3.77	26.44	75.48	67.71	19.92	0.66	1.97
Pt^{+4}	3.36	2.63	67.28	52.60	17.38	44.20	1.68	1.32
Mixed Above	1.03	1.54	20.62	30.84	74.82	67.28	0.52	0.77

A: Amount of adsorbed Mo(VI) (mg/L), $L=C_e^{No\text{-}ion}-C_e/C_e^{No\text{-}ion}$: Loss adsorption (%), $E=C_0-C_e/C_0$: extraction percentage (%) and $D=Q/C_e$: distribution ratio

3.10. Analysis of the real samples.

To examine the ability of the adsorbent under optimal conditions (the best pH values, 0.01g-25mL), we have estimated the adsorption of the ions with 0.2, 0.4 and 0.6 mg/L in various environmental aqueous samples. Table 6 shows the results of recovery (Mean and SD) of two different samples under the similar conditions with high recovery in which is defined as follows.

$$Recovery_{(N+1)}\% = \frac{C_{Found(N+1)}}{C_{Spiked(N+1)} + C_{Found(N)}} \times 100 \quad (9)$$

Table 6. Results of Mo(VI), Pd(II) recovery after spiking in various water samples

Samples Water	Found (without spiking of ion ($\mu g.mL^{-1}$)		Added ion ($\mu g.mL^{-1}$)		Found ion, after pre-conc. ($\mu g.mL^{-1}$) [a]		Recovery (%)		Relative standard deviation (%)[a]	
	Mo(VI)	Pd(II)	Mo(VI)	Pd(II)	Mo(VI)	Pd(II)	Mo(VI)	Pd(II)	Mo(VI)	Pd(II)
Tap Water	0.25	0.21	0.2 0.4 0.6	0.2 0.4 0.6	0.46 0.66 0.86	0.43 0.63 0.82	97.12 98.48 98.46	96.09 96.82 98.78	3.30 3.03 1.77	3.58 1.58 2.11
Well Water	0.12	0.15	0.2 0.4 0.6	0.2 0.4 0.6	0.33 0.53 0.75	0.34 0.55 0.77	96.00 98.73 98.63	101.94 100.61 97.40	4.58 2.19 4.94	4.45 3.81 1.30

a: For three determinations

4. Conclusions

According to the results obtained in this project, significant points can be shown in connection with the operational nanotubes and their adsorption of Pd (II) and Mo (VI) ions:

1- The results of examining the relationship between the adsorption percentage and initial concentrations show interesting differences. For example, it has been shown that the percent of Mo(VI) and Pd(II) adsorption through nanotubes depends on their initial concentrations in the solution. The adsorption percentage concentrations of about 2 mg/L for palladium ions and 1 to 2 mg/L for molybdenum ions. The different optimal pH and the initial concentrations for the two ions can be successfully used for separation of these ions from each other. In addition, the difference in behavior of different detergents increases the chances of achieving this goal.

2- The table of the ion adsorption time shows that the behavior of ions in the adsorption rate is different, which can be taken into account and used.

3- Examination of the percentage of saturation of synthesized nanotubes at different times shows that the percentage of saturation increased over time and was then detected (approximately 120 minutes). The adsorption capacity of functionalized nanotubes was also calculated at different concentrations for two ions and increased with increasing ion concentration.

Acknowledgements

The authors would like to acknowledge all those who aided in this work, and the nuclear science and technology research institute for financial and technical supports.

References

- Thunderer, M., Toxicological information on single compounds, metals 3; 14th ed. Landsberg, Ecomed, 1994, p. 1 (in German).
- Edelmetall Taschenbuch der Degussa AG, 2nd edn. (Hüthig, Heidelberg 1995)
- Deichmann, W.B.; Le-Blanc, T.J. Determination of the approximate lethal dose with about six animals. J Ind Hyg Toxicol, 1943 25:415–417
- Cotton, F. A.; Wilkinson, G. Inorganic nchemistry: an advanced summary, 4th ed. Weinheim, Verlag Chemie, 1982, 917–981 (in German).
- Cowley, A. "Platinum"; London, Johnson Matthey plc, 1997, 35- 50.
- Cowley, A. "Palladium"; London, Johnson Matthey plc, 1999, 31-32
- Sutulov, A.International Molybdenum Encyclopaeia, Vol. 2, Intermet Publications, Santiago, Chile, 1979. p. 296.
- Accina, D. J. J. Palladium-Ruthenium Alloys, Metals Handbook, 9th Edition, Vol. 2, American Society for Metals, Metals Park, Ohio, 1979,p.771.
- Aerospace Structural Metals Handbook, Mechanical Properties Data Center, Department of Defense, Belfour Stulen, Inc., Code 5301, Mar. 1963, p. 5. 7.
- Kummer, J. T. "Molybdenum"; Mineral Commodity Profiles, U. S. Dept. of the Interior, Bureau of Mines, 1979.
- Archer, R. S.; Briggs, J. Z.; Loeb, C. M. Molybdenum Steels-Irons-Alloys, Climax Molybdenum Company, NewYork.1948.
- Marshall, M.W.; Popa-Nita, S.; Shapter, J.G. Measurement of functionalized carbon nanotubes carboxylic acid groups using a simple chemical process. Carbon 2006, 44, 1137-1141,
- Haroun, A.A.; Mossa, A.H.; Mohafrash, S.M. Preparation and biochemical evaluation of functionalized multi-walled carbon nanotubes with Punica granatum extract. Curr Bioactive Comp. 2019, 15, 138-144,
- Haroun, A.A.; Amin, H.A.; Abd El-Alim, S.H. Preparation, Characterization and In vitro

biological activity of soyasapogenol B loaded onto functionalized multi-walled carbon nanotubes. Curr Bioactive Comp. 2018, 14, 364-372,

- Amin H.A., Haroun A.A. Comparative studies of free and immobilized Aspergillus flavus onto functionalized multi-walled carbon nanotubes for soyasapogenol B production. Egypt Pharma J. 2017, 16, 38-143,
- Khaled, E.; Kamel, M.S.; Hassan, H.N.A.; Haroun, A.A.; Youssef, A.M.; Aboul-Enein, H.Y. Novel multiwalled carbon nanotubes/β-cyclodextrin based carbon paste electrode for flow injection potentiometric determination of piroxicam. Talanta 2012, 97, 96-102
- Mubarak, N.M.; Wong, J.R.; Tan, K.W.; Sahu, J.N.; Abdullah, E.C.; Jayakumar, N.S.; Ganesan, P. Immobilization of cellulase enzyme on functionalized multiwall carbon nanotubes. J. Molecular Catalysis B: Enzymatic 2014, 107, 124-131,
- Shah, S.; Solanki, K.; Gupta, M.N. Enhancement of lipase activity in non-aqueous media upon immobilization on multiwalled carbon nanotubes. Chem Central J. 2007, 1,1-6
- Pavlidis, I.V.; Tsoufis, T.; Enotiadis, A.; Gournis, D.; Stamatis, H. Functionalized multi-wall carbon nanotubes for lipase immobilization. Adv. Eng. Mater. 2010, 12, 179-183,
- Pathania, D.; Sharma, S.; Singh, P. Removal of methylene blue by adsorption onto activated carbon developed from Ficus carica bast. Arab J Chem 2017, 10, S1445-S1451,
- Vishali, S.; Mullaim P. Analysis of two-parameter and three-parameter isotherms by nonlinear regression for the treatment of textile effluent using immobilized Trametes versicolor: comparison of various error functions. Desalin Water Treat 2016, 57(56), 27061–27072
- 22 Kumar, K.V. Comparative analysis of linear and non-linear method of estimating the sorption isotherm parameters for malachite green onto activated carbon, J. Hazard. Mater.2006, 136, 197–202.
- Kumar,. K.V.; Porkodi, K.; Rocha, F. Isotherms and thermodynamics by linear and non-linear regression analysis for the sorption of methylene blue onto activated carbon: comparison of various error functions, J. Hazard. Mater.2008, 151,794–804.